

DESIGN CRITERIA FOR INFLATED, EXPANDABLE BEAMS USED AS
STRUCTURAL MEMBERS IN AN ADVANCED CONCEPT PARAGLIDER

By Royce A. Toni and James F. McNulty

NASA Langley Research Center

INTRODUCTION

As a result of the interest shown in an inflatable paraglider for possible application as a device for suitable payload recovery, it has been necessary to develop the engineering tools to perform a structural design of the inflated members associated with the load transfer from the aerodynamic membrane to the shroud lines. The basic problem is to provide a minimum weight design while still assuring that the members will not buckle or burst under load.

Design procedures have been developed which allow inflated curved beams to be designed with due consideration being given to concentrated and distributed loads acting in arbitrary planes. Paragliders designed by methods outlined herein have been tested in wind tunnels under varying aerodynamic loading conditions and have been found to exhibit buckling tendencies near the load condition predicted analytically.

This paper concerns itself primarily with the analytical design procedures to be utilized after the loading condition has been established. The determination of the loading conditions on the structural members, either experimentally or analytically, is an interesting but separate problem.

SYMBOLS

A	leading-edge and keel cross-sectional area equal to $2\pi r$, in.
A _e	leading-edge axial compression depicted in figure 2 under section A-A as accumulative effects along member's length and shown vectorially according to right-hand rule in figure 4, lb
A _k	keel axial compression depicted in figure 2 under section C-C as accumulative effects along member's length and shown vectorially according to right-hand rule in figure 5, lb
E	Young's modulus of elasticity for fabric, lb/in.
F	fabric breaking strength, lb/in.
I	leading-edge and keel cross-section moment of inertia, in. ³

Report Documentation Page			Form Approved OMB No. 0704-0188		
Public reporting burden for the collection of information is estimated to average 1 hour per response, including the time for reviewing instructions, searching existing data sources, gathering and maintaining the data needed, and completing and reviewing the collection of information. Send comments regarding this burden estimate or any other aspect of this collection of information, including suggestions for reducing this burden, to Washington Headquarters Services, Directorate for Information Operations and Reports, 1215 Jefferson Davis Highway, Suite 1204, Arlington VA 22202-4302. Respondents should be aware that notwithstanding any other provision of law, no person shall be subject to a penalty for failing to comply with a collection of information if it does not display a currently valid OMB control number.					
1. REPORT DATE 1965		2. REPORT TYPE		3. DATES COVERED 00-00-1965 to 00-00-1965	
4. TITLE AND SUBTITLE Design Criteria for Inflated, Expandable Beams Used as Structural Members in an Advanced Concept Paraglider				5a. CONTRACT NUMBER	
				5b. GRANT NUMBER	
				5c. PROGRAM ELEMENT NUMBER	
6. AUTHOR(S)				5d. PROJECT NUMBER	
				5e. TASK NUMBER	
				5f. WORK UNIT NUMBER	
7. PERFORMING ORGANIZATION NAME(S) AND ADDRESS(ES) Wright Air Development Center,Wright Patterson AFB,OH,45433				8. PERFORMING ORGANIZATION REPORT NUMBER	
9. SPONSORING/MONITORING AGENCY NAME(S) AND ADDRESS(ES)				10. SPONSOR/MONITOR'S ACRONYM(S)	
				11. SPONSOR/MONITOR'S REPORT NUMBER(S)	
12. DISTRIBUTION/AVAILABILITY STATEMENT Approved for public release; distribution unlimited					
13. SUPPLEMENTARY NOTES					
14. ABSTRACT see report					
15. SUBJECT TERMS					
16. SECURITY CLASSIFICATION OF:			17. LIMITATION OF ABSTRACT	18. NUMBER OF PAGES 18	19a. NAME OF RESPONSIBLE PERSON
a. REPORT unclassified	b. ABSTRACT unclassified	c. THIS PAGE unclassified			

I_x	leading-edge and keel cross-section moment of inertia with respect to x axis, in. ³
I_y	leading-edge and keel cross-section moment of inertia with respect to y axis, in. ³
J	leading-edge and keel cross-section polar moment of inertia, in. ³
K	strength-to-weight ratio of fabric, lb/in./oz/yd ²
M_e	leading-edge vertical bending moment depicted in figure 2 under section A-A, and shown vectorally according to right-hand rule in figure 4, ft-lb
$(M_e)_I$	leading-edge inboard bending moment depicted in figure 2 under section B-B, and shown vectorally according to right-hand rule in figure 4, ft-lb
(M_k)	keel vertical bending moment depicted in figure 2 under section C-C, and shown vectorally according to right-hand rule in figure 5, ft-lb
M_R	leading-edge resultant bending moment equal to $\sqrt{(M_e)^2 + [(M_e)_I]^2}$ shown vectorally according to right-hand rule in figure 4, ft-lb
n_o	burst preventive safety factor, unitless
"O"	that point on structural member's cross section where stress is critical due to bending (refer to figs. 4 and 5)
p	inflation pressure, lb/in. ²
Q	static moment of inertia of arc, in. ²
r	structural member inflated radius, in.
r_f	fabricated radius for an inflated beam, in.
S	length along arc of a circle, in.
V_e	leading-edge vertical shear depicted in figure 2 under section A-A, and also shown in figure 4, lb
$(V_e)_I$	leading-edge inboard shear depicted in figure 2 under section B-B, and also shown in figure 4, lb
V_k	keel vertical shear depicted in figure 2 under section C-C, and also shown in figure 5, lb
W	fabric weight, oz/yd ²

x,y	Cartesian coordinate system for a structural member's cross section with a positive sense shown in figure 3
Z	torque, ft-lb
Z _e	leading-edge torque, ft-lb
ε	strain for an inflated material, in./in.
ρ	perpendicular distance from centroid of an area to its axis of inertia, in.
σ _H	hoop stress, lb/in.
σ _L	longitudinal stress, lb/in.
τ _O	resulting shear stress at point "O," lb/in.
τ _V	shear stress, lb/in.
τ _Z	torsional stress, lb/in.
τ _{cr}	critical shear stress equal to $\sqrt{\sigma_H \sigma_L}$, lb/in.
θ	angular direction along circumference of structural member's cross section with a positive sense as shown in figure 3, deg
θ ₁	angle locating some arbitrary point on structural member's cross section (refer to fig. 3), deg
ω	angle defined as $\tan^{-1} \frac{M_e}{(M_e)_I}$ (refer to fig. 4), deg

DESCRIPTION OF AN ADVANCED CONCEPT PARAGLIDER

A paraglider, simply speaking, is a flying wing which has glide and maneuver capability through adjustment of the shroud line lengths which locates the payload relative to the resultant aerodynamic lift vector; this, in turn, determines the glide and sideslip angle. According to reference 1, an inflatable paraglider would be classified as that type expandable structure which employs the use of internal gas pressurization to provide the energy for deployment and then is dependent upon the same pressurization to maintain the paraglider in its deployed shape.

Once deployed and pressurized the advanced concept paraglider takes on the shape illustrated in figure 1. The leading edges and keel serve as the structural members and are joined at the apex; thus, in effect they represent a structural frame composed of inflated fabric beams. The space vehicle is slung beneath the paraglider and connected to it by shroud lines, or

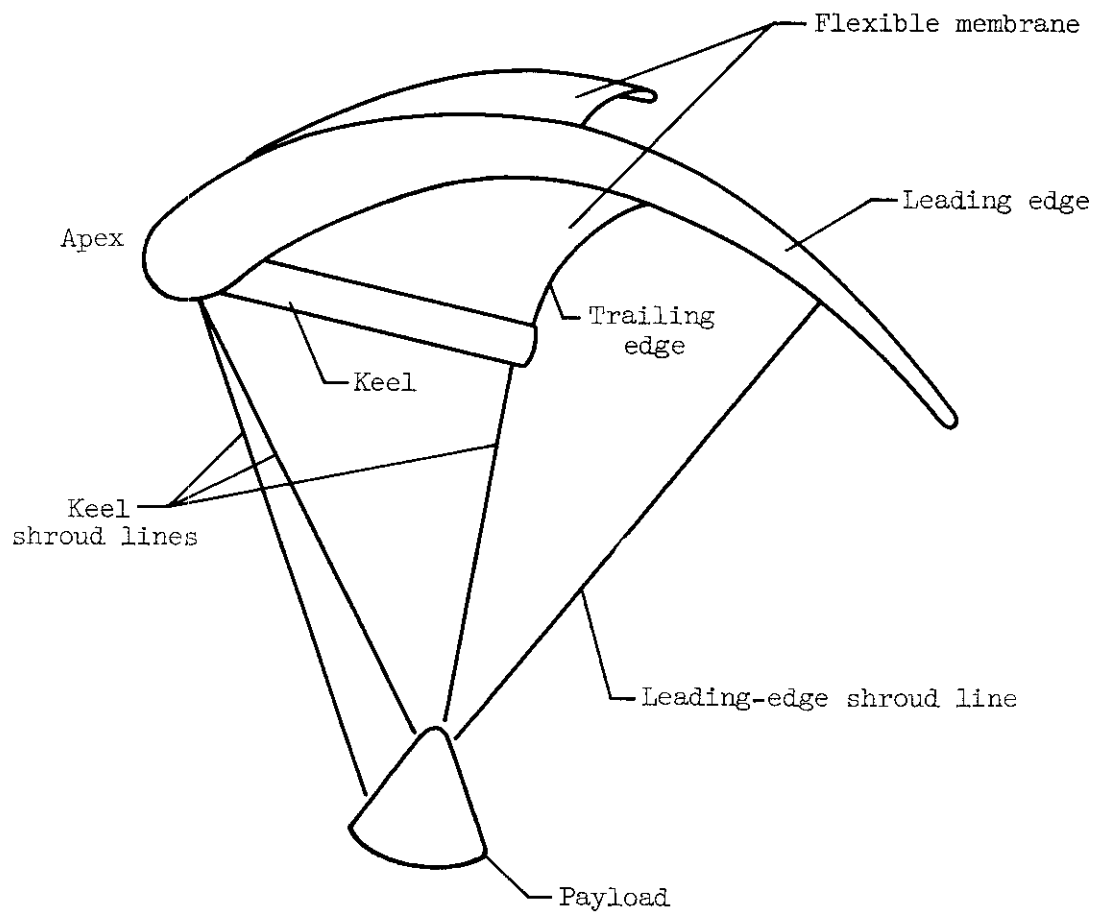


Figure 1.- A deployed advanced concept paraglider.

cables. The number of cables directly affects the imposed loads acting upon the structural members. The more cables, the less critical become the effect of the loads; however, at the same time the expectancy for successful deployment is reduced. Thus, a trade-off must be made. It was felt that the arrangement of three cables from the keel (two at the apex and one at the aft end) and one cable from each of the leading edges (at the three-quarter points) provided sufficient stability and structural integrity while keeping the complexities of the deployment to a minimum.

In the advanced concept, high-aspect-ratio paraglider, the longitudinal shape of the leading-edge center line is curved, approximating an arc of a circle while its circular cross section varies linearly from a relatively large diameter at the apex to a small diameter at the tip. The keel is considerably shorter in length and maintains a constant-diameter circular cross section. Physically the advanced concept paraglider differs from the conventional concept in that the latter has three structural members of constant circular cross section, equal in length and lying in the same plane.

Attached between the leading edges and keel is the membrane. That part of the membrane running from tip to tip of each structural member is termed the trailing edge. The membrane is entirely flexible and assumes a shape governed by the aerodynamic pressure.

The primary advantage of the advanced concept paraglider is that it offers a relatively marked increase in glide characteristics over the conventional concept by reducing the drag; thus, the advanced concept would have the flexibility to glide to more distant landing sites.

LOAD AND MOMENT DEFINITION

Paraglider design is hindered by an inability to define theoretically the load distributed to the leading edges and keel due to aerodynamic pressure acting on the membrane. This difficulty is created by both the flexibility of the membrane (it changes its shape with every maneuver as does the magnitude of the load distribution) and the difficulty of defining the direct aerodynamic load on the structural members themselves.

In an attempt to circumvent the aforementioned difficulty, Langley Research Center initiated a program that incorporated the use of a high-aspect-ratio, rigid paraglider model fitted with load and moment measuring balances. The model was wind-tunnel tested over a range of angles of attack. The resulting load and moment coefficients were recorded and plotted for each structural member for various stations along its length. Since the balances were multicomponent it was possible to record any desired force at these stations in three perpendicular planes. The same loads model configuration was compatible with models investigated for aerodynamic performance at various angles of attack. From the aerodynamic study, the paraglider's glide and flare angles of attack were selected; the data from the loads model for these angles of attack were then used as design inputs.

The resulting loads for the glide angle of attack served as the design criteria for the structural members in dictating member deflections so as to

achieve the desired in-flight shape. Those loads for the flare angle of attack, corrected for a conservatively assumed 1.5g load factor, dictated the leading-edge internal pressure requirements to resist wrinkling. The pressure was then selected for the entire vehicle and served as the basis for arriving at a keel radius.

The inertia loads were taken into consideration by initially assuming the weights of the structural members and distributing them along the member's length to a second-order approximation for the leading edge (since its cross section tapers with length) and a uniform distribution for the keel (since its cross section is constant with length).

The shroud line loads were distributed in accordance with elastic bending theory (the actual mechanics are beyond the scope of this paper). Thus, the aerodynamic, inertia, and shroud line loads all contributed to the total effective imposed loads acting upon the structural members.

For the advanced concept paraglider considered herein the leading-edge geometry was governed by aerodynamic considerations. The design loads and moments shown in figure 2 were determined in the manner outlined above.

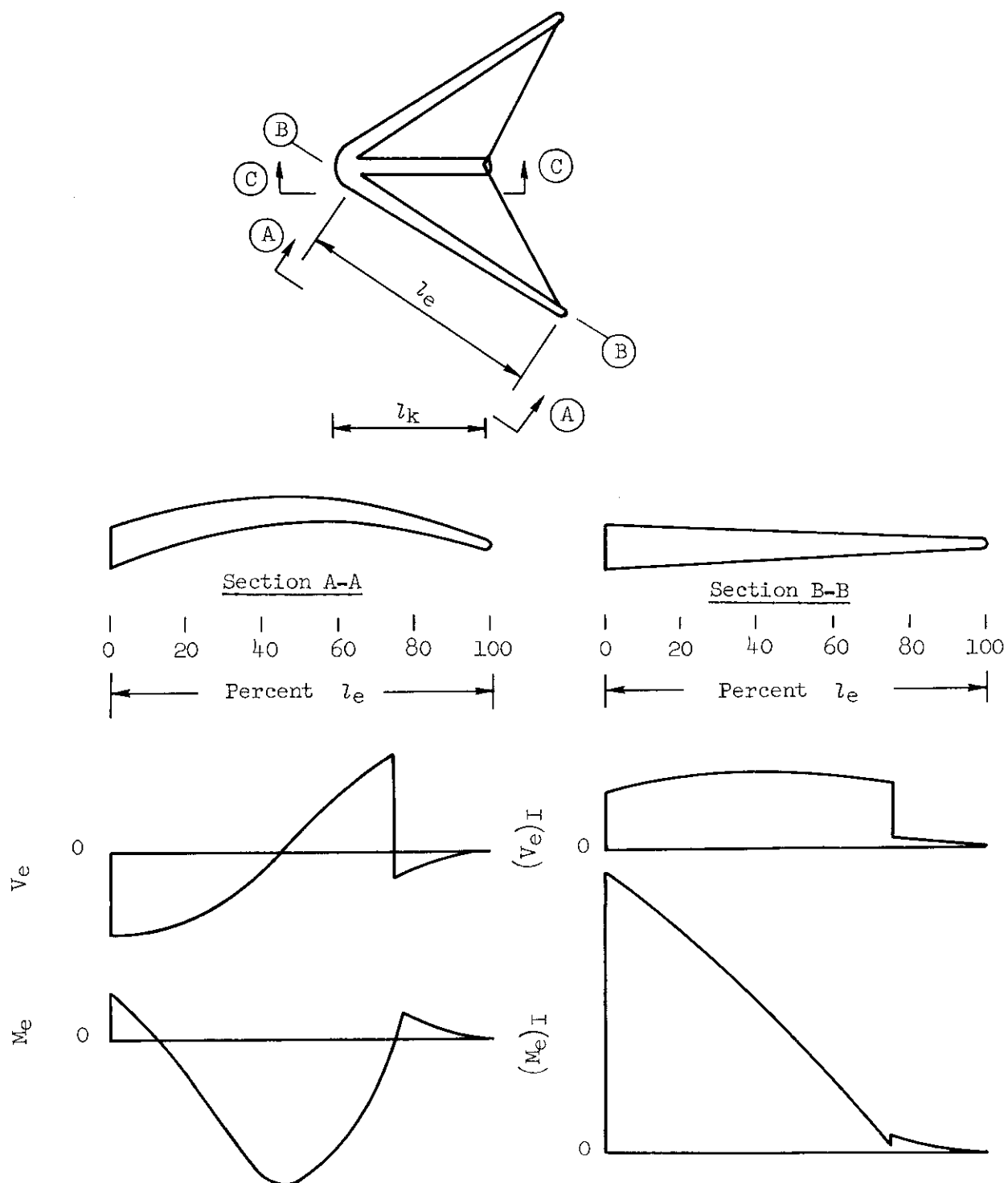
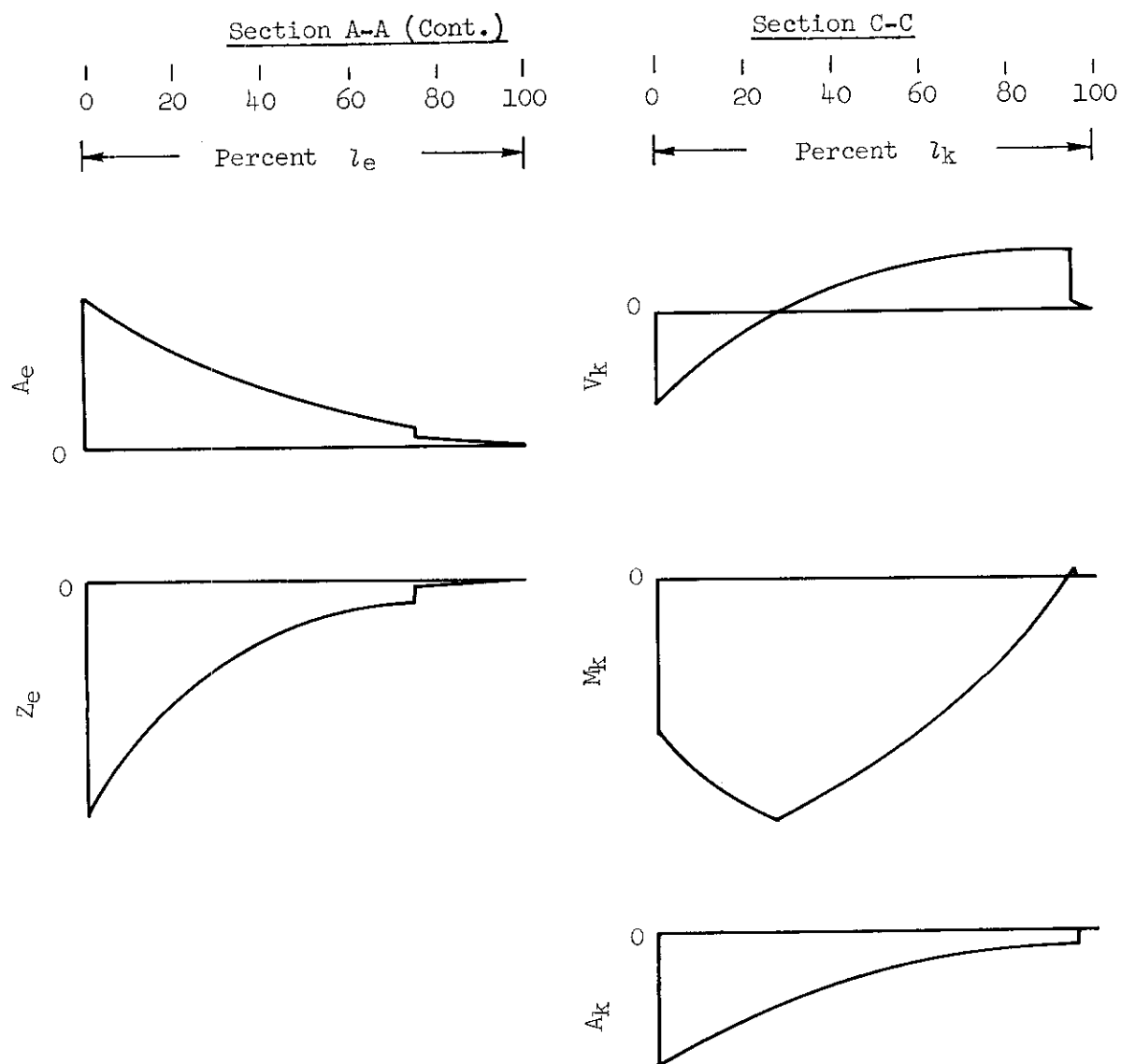


Figure 2.- The resulting imposed load shapes on the structural members of a prototype advanced concept paraglider of aspect ratio 5.4 with a flare angle of attack of 23° and a 1.5 load correction factor.



NOTE: A_e and A_k are the leading-edge compression and the keel tension, respectively, and are shown as accumulative effects along the member's length.

Z_e is the leading-edge torque and is positive in direction when looking down leading edge from tip to apex.

Section B-B is a plan view of the leading edge.

Figure 2.- Concluded.

BASIC EQUATIONS USED IN INFLATABLE BEAM DESIGN

This section pertains to the derivation of equations applicable for design of a circular cross section, inflated fabric beam. Figure 3 shows the typical cross section for such a beam and will be referred to in deriving the expressions for area, moment of inertia, static moment of inertia of arc, and torsional shear stress. The cross section is considered a ring with a thickness t negligible in comparison with radius r . As is customary with fabric design procedures, stress is expressed as lb/in. of fabric, I as in.³, and A as inches; thus, t is omitted as a parameter.

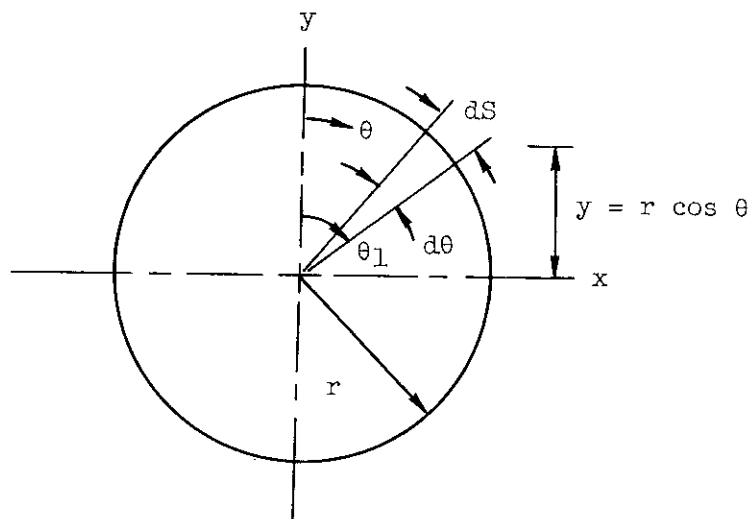


Figure 3.- Cross section of inflated fabric beam.

1. Area

$$A = \int dA \quad (1)$$

For the area associated with $d\theta$ in figure 3

$$A = \int_{\theta_1 - d\theta}^{\theta_1} r \, d\theta \quad (2)$$

Integrating for the complete ring results in:

$$A = 2\pi r \quad (3)$$

2. Moment of Inertia

The mathematical definition of moment of inertia is stated in the following expression:

$$I = \int \rho^2 dA \quad (4)$$

where ρ is the perpendicular distance from the differential area dA , to the axis of inertia. For the case illustrated in figure 3 the following is true

$$I_x = I_y \quad (5)$$

and considering the x axis as the axis of inertia yields

$$I_x = \int_{\theta_1-d\theta}^{\theta_1} y^2 dA \quad (6)$$

By substituting an expression for y , in terms of r and θ , into equation (6) along with the assumption

$$dS = r d\theta = dA \quad (7)$$

and integrating over the entire cross section, the following expression is arrived at

$$I_x = 4r^3 \int_0^{\pi/2} \cos^2 \theta d\theta \quad (8)$$

Performing the indicated definite integration yields the equation for the moment of inertia. Thus,

$$I_x = \pi r^3 \quad (9)$$

3. Static Moment of Inertia of Arc

By definition the static moment of inertia of an area is the product of that area and its perpendicular distance from the natural axis. Thus, for the differential area illustrated in figure 3,

$$dQ = \int_{\theta_1-d\theta}^{\theta_1} y dA \quad (10)$$

Substituting the expression for y and dA into the above, and expressing the integral for that part of the arc above the neutral axis yields

$$Q = 2r^2 \int_0^{\pi/2} \cos \theta \, d\theta \quad (11)$$

Performing the indicated definite integration results in the expression for the static moment of inertia of arc or,

$$Q = 2r^2 \quad (12)$$

4. Torsional Shear Stress

Torsional shear stress for a circular cross section in the form of an equation is simply stated as

$$\tau_z = \frac{Zr}{J} \quad (13)$$

where Z is the torque and J the polar moment of inertia. The polar moment of inertia is defined as

$$J = I_x + I_y \quad (14)$$

and substituting equation (5) into the above yields the polar moment of inertia for a circular cross section.

$$J = 2I_x \quad (15)$$

Now replacing I_x by equation (9) results with J ,

$$J = 2\pi r^3 \quad (16)$$

Substituting the above into equation (13) yields an expression for the torsional shear. Thus,

$$\tau_z = \frac{Z}{2\pi r^2} \quad (17)$$

DESIGN OF STRUCTURAL FRAME MEMBERS

Once the imposed loads are established for the structural members it is possible to arrive at the inflation pressure for the leading edge followed by determining the radius for the keel. The engineering concept employed was

developed by the authors in collaboration with Goodyear Aerospace engineers* under NASA Contract NAS1-3020.**

1. The Leading-Edge Structural Member

In considering the leading edge a cross section subjected to the imposed loads is shown in figure 4. From figure 4 it can be seen that,

$$\omega = \tan^{-1} \frac{M_e}{(M_e)_I} \quad (18)$$

$$M_R = \sqrt{M_e^2 + (M_e)_I^2} \quad (19)$$

$$V_2 = V_e \cos \omega - (V_e)_I \sin \omega \quad (20)$$

$$V_1 = (V_e)_I \cos \omega + V_e \sin \omega \quad (21)$$

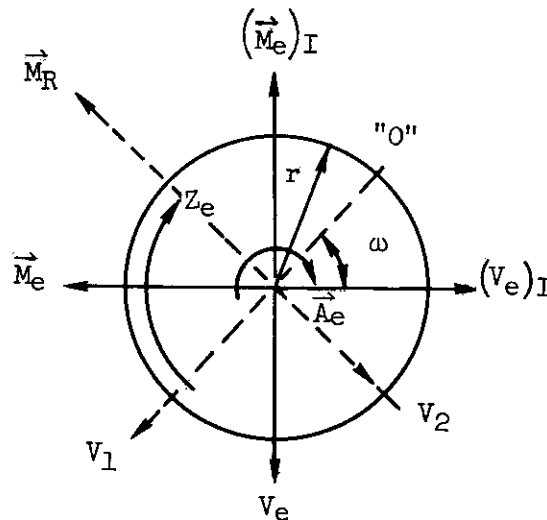


Figure 4.- Leading-edge cross section under imposed loads (looking from tip toward apex).

*B. W. Raff and T. L. Hoffman.

**This contract represents one phase of the research currently under investigation by Langley Research Center concerning inflatable paragliders, and it pertains primarily to a recovery system for manned space vehicles using an Apollo-type capsule. Goodyear Aerospace Corporation of Akron, Ohio, was the contractor.

The point "0" represents that point on the cross section where the stress is critical for buckling due to the resultant bending moment M_R . Also at that point the value of the shear stress is zero due to V_1 and maximum due to V_2 . The shear stress due to torsion is constant around the ring.

If the inflation pressure is symbolized by p , then the normal stresses are given by

$$\sigma_H = pr \quad (22)$$

$$\sigma_L = p \frac{r}{2} - \frac{A_e}{A} - \frac{M_R r}{I} \quad (23)$$

(The above equation takes into consideration the effect of combined stresses, including the influence of inflation pressure. It is in this respect that the design concept differs from the more conventional practice which deals with noninflative type structures.)

Making substitutions for A and I into equation (23) results with

$$\sigma_L = \frac{\pi pr^3}{2\pi r^2} - \frac{A_e r}{2\pi r^2} - \frac{2M_R}{2\pi r^2} \quad (24)$$

The shear stress due directly to V_2 for a ring can be stated as

$$\tau_V = \frac{V_2 Q}{2I} \quad (25)$$

and making the proper substitutions for Q and I yields

$$\tau_V = \frac{2V_2 r}{2\pi r^2} \quad (26)$$

The shear stress due to torsion was derived in the previous section as

$$\tau_Z = \frac{Z_e}{2\pi r^2} \quad (27)$$

The resulting shear stress at point "0" is the difference between the shear stress due to V_2 and the shear stress due to torsion, or stated in the form of an equation,

$$\tau_0 = \frac{2V_2 r - Z_e}{2\pi r^2} \quad (28)$$

Reference 2, page 21, shows the expression for critical shear stress in terms of the normal stresses as being

$$\tau_{cr} = \sqrt{\sigma_H \sigma_L} \quad (29)$$

The critical shear stress is defined as the shear stress which causes one principal stress to go to zero (i.e., causes wrinkling in the members). Thus, if the shear stress in equation (28) is made equal to the critical shear stress, the state of incipient buckling at point "0" is defined. From squaring both sides of equation (29) comes the expression

$$(\tau_{cr})^2 = \sigma_H \sigma_L \quad (30)$$

Substituting equations (22), (24), and (28) into equation (30) yields

$$\left(\frac{2V_2 r - Z_e}{2\pi r^2} \right)^2 = \frac{pr(\pi p r^3 - A_e r - 2M_R)}{2\pi r^2} \quad (31)$$

Simplification of the above equation and use of the quadratic formula yields a workable expression for determining p .

$$p = \frac{A_e r + 2M_R \pm \sqrt{(A_e r + 2M_R)^2 + (2V_2 r - Z_e)^2}}{2\pi r^3} \quad (32)$$

Thus, p is determined based upon the interactional effects of shear, bending moment, axial forces, and torque. Values of the aforementioned forces at various increments along the beam can be substituted into equation (32) yielding a range of inflation pressures. The maximum yielded inflation pressure from this range is selected as the inflation pressure for the structural system and assures that no point on the structural members will wrinkle due to a compressive stress since this was postulated by use of equation (29). It now readily follows that a fabric can be selected which assures that burst will not occur by applying a safety factor to the hoop load (pr).

2. The Keel Structural Member

In considering the keel the problem is altered somewhat in that the inflation pressure is known and emphasis is placed upon determining the radius, which in this case is constant throughout the member's length. A keel cross section subjected to the imposed loads is shown in figure 5.

The point "0" is that point on the keel cross section where the stress is critical for buckling due to the bending moment M_k . It can be seen that the shear stress at "0" due to V_k is zero, and also, that there is no torsional stress.

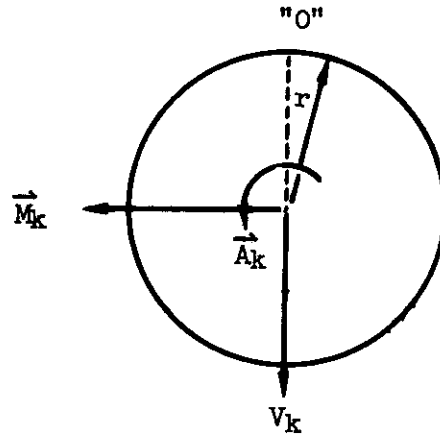


Figure 5.- Keel cross section under imposed loads (looking from tip toward apex).

The normal stresses are given by

$$\sigma_H = pr \quad (33)$$

$$\sigma_L = \frac{pr}{2} + \frac{A_k}{A} - \frac{M_k r}{I} \quad (34)$$

It should be noted that equation (33) differs from equation (22) in that the involved radii are not the same. Also in equation (34) the direction of the axial load A_k is opposite to that of the leading edge. When substitutions are made for A and I in equation (34) the expression becomes

$$\sigma_L = \frac{\pi pr^3 + A_k r - 2M_k}{2\pi r^2} \quad (35)$$

Since the point "O" is critical and there are no shear stresses at this point, the critical shear stress is zero and equation (29) yields

$$\sigma_H \sigma_L = 0 \quad (36)$$

Substituting equation (35) into the above gives a third-order expression from which r can be solved.

$$\pi pr^3 + A_k r - 2M_k = 0 \quad (37)$$

It can be seen that the radius of the keel is a function of the inflation pressure, bending moment, and axial forces. Knowing the inflation pressure, and substituting values of the involved forces at various increments along the beam into equation (37) yields a range of radii. The maximum radius from this range is selected as the radius of the keel structural member.

EFFECT OF INFLATIVE GROWTH AND BURST ON FABRICATED RADIUS

Since the structural member will "grow" in size when inflated owing to the hoop strain, it is therefore essential the member be fabricated to a lesser diameter so that, at operating conditions, the configuration will accurately depict the desired aerodynamic geometry.

In accordance with fabric terminology the modulus of elasticity E is measured in pounds/inch. If r_f represents the fabricated radius, then from Hooke's Law,

$$\text{Growth in circumference} = \frac{2\pi r_f p r_f}{E} \quad (38)$$

If the desired aerodynamic radius (the radius the structural member achieves once inflated) is designated r then equation (38) can be rewritten as

$$2\pi r - 2\pi r_f = \frac{2\pi r_f p r_f}{E} \quad (39)$$

from which

$$r = r_f \left(\frac{p r_f}{E} + 1 \right) \quad (40)$$

But

$$\epsilon = \frac{p r_f}{E} \quad (41)$$

and substituting equation (41) into (40) results in

$$r_f = \frac{r}{1 + \epsilon} \quad (42)$$

Thus the member should be fabricated to the radius given by equation (42).

It now readily follows that a fabric can be selected which assures that burst will not occur by applying a safety factor n_0 to the hoop load $p r_f$. That is to say, the required material strength is defined as

$$F = n_0 p r_f \quad (43)$$

Replacing r_f in the above expression with equation (42) gives

$$F = n_0 p \left(\frac{r}{1 + \epsilon} \right) \quad (44)$$

If the strength-to-weight ratio of the material is designated K , then

$$K = \frac{F}{W} \quad (45)$$

and

$$F = KW \quad (46)$$

Substituting the above expression into equation (44) yields an expression for the desired material weight.

$$W = \frac{n_o pr}{K(1 + \epsilon)} \quad (47)$$

Thus equation (47) represents the governing equation for the selection of material based upon weight requirements, where the weight is expressed as a function of the burst safety factor, inflation pressure, strength-to-weight ratio, strain, and inflated radius. In addition, it is noted that the selected fabric should have equal strength in the hoop and meridional directions since, at the point of maximum stress in the meridional direction the pressure stress and tension bending stress combine to equal the stress in the hoop direction.

CONCLUDING REMARKS

For an advanced concept paraglider whose inflatable structural frame is composed of curved tapered leading edges and a cylindrical keel, analytical formulas are presented in the paper which will allow, for defined load conditions, the determination of:

(1) The required pressurization to assure that the leading edges will not buckle under load.

(2) The diameter required for the keel, compatible with the internal pressurization, which assures that the keel will not buckle under load.

In addition to the above, methods are included on selecting fabric strengths to safeguard the frame against burst and on defining the frame's fabricating size so that, under pressurization growth, the frame will assume the desired aerodynamic size.

REFERENCES

1. Forbes, F. W.: Expandable Structures. Space/Aeronautics, Dec. 1964, pp. 62-68.
2. Introduction to Structural Analysis of Expandable Structures. GER-9870.
3. Hoffman, T. L.; and Raff, B. W.: Advanced Concept Inflatable Paraglider Prototype and Model Design. Contract No. NAS1-3020, GER-11520.
4. Singer, Ferdinand L.: Strength of Materials. Harper and Brothers Publishers, New York, 1951, ch. 5.
5. Singer, Ferdinand L.: Engineering Mechanics. Harper and Brothers Publishers, New York, 1954, Second Edition, ch. 8.